33rd Annual International Conference of the IEEE EMBS
Boston, Massachusetts USA, August 30 - September 3, 2011

A Novel Unsupervised Spike Sorting Algorithm for Intracranial EEG

R. Yadav[1], *Student Member, IEEE*, A. K. Shah[2], J. A. Loeb[2,3], M. N. S. Swamy[1], *Fellow, IEEE,* and R. Agarwal[1], *Member, IEEE*

***Abstract*—This paper presents a novel, unsupervised spike classification algorithm for intracranial EEG. The method combines template matching and principal component analysis (PCA) for building a dynamic patient-specific codebook without *a priori* knowledge of the spike waveforms. The problem of misclassification due to overlapping classes is resolved by identifying similar classes in the codebook using hierarchical clustering. Cluster quality is visually assessed by projecting inter- and intra- clusters onto a 3D plot. Intracranial EEG from 5 patients was utilized to optimize the algorithm. The resulting codebook retains 82.1% of the detected spikes in non-overlapping and disjoint clusters. Initial results suggest a definite role of this method for both rapid review and quantitation of interictal spikes that could enhance both clinical treatment and research studies on epileptic patients.**

***Index Terms*—EEG, interictal spike, clustering, PCA**

I. Introduction

PATIENTS with medically refractory epilepsy are often candidates for resective surgery when they fail to respond to medications. In order to guarantee a good outcome, it is critical that regions of the brain that produce seizures and epileptic activities are identified. These patients undergo prolonged intracranial EEG monitoring that allows neurophysiologists to determine seizure foci and other areas that show interictal epileptic activities or spikes. Prolonged EEG monitoring, can last from a few to many days and generates a massive amount of data. Visual review of such voluminous data for spike and seizure detection is very tiresome, laborious, expensive, and lacks quantitation. For this reason, automatic spike and seizure detection techniques have received intense attention. Although, automatic methods significantly reduce review time, their performance is still not acceptable to the well-trained EEGers.

Several studies report a better surgical outcome when removing regions of frequent interictal spikes in addition to the regions of seizure onset [1], [2]. However, exactly how interictal spikes develop and how they propagate and contribute to the generation of seizures is not well understood [1], [3]. A recent study examined human brain tissues at regions of seizure onset and defined a small group of genes that are highly correlated with the interictal spike frequency [4], [5]. Thus, both qualitative and quantitative analysis of interictal spiking is not only important for patient management, but may also help identify epileptic biomarkers and drug targets.

Spike sorting is the first step in the qualitative and quantitative analysis of interictal spikes. The process involves detecting spikes, and clustering or mapping each spike to its source. Spike sorting is generally considered a high dimensional clustering problem that still remains incompletely-solved due to issues of nonstationarity, non-Gaussianity, and temporal dependencies between spikes [6]-[12]. In addition, classifying spikes directly from the recorded waveforms in high dimensional space is challenging because data points would be sparse, and clustering algorithms tend to be imprecise [7], [13], [14]. Correcting sorting errors manually thus becomes mandatory, which is time-intensive and subjective [14]. Furthermore, complexity of spike sorting increases in clinical situations where up to 128 electrodes are sampled simultaneously for many days. Note that a small EEG section can contain thousands of interictal spikes. Therefore, computationally light, accurate and robust spike sorting methods to reduce the load of manual spike sorting are sought.

Several spike-sorting methods exist in the literature that are specifically designed for scalp EEG. These are limited to a few channels and require the knowledge of complete recording prior to classification. Template-based matching methods report a superior performance over other techniques. These methods mainly employ principal component analysis (PCA) and wavelet transformations to generate spike templates from all spikes in the recording [6], [12].

One of the major challenges in online spike sorting methods arises due to a wide variety of spike waveforms and the lack of *a priori* knowledge of spike information for each patient. The large number of electrodes introduces computational complexity which can vary from patient to patient. Furthermore, the EEG is digitized at different sampling rates (200 to 1000 Hz) within the same centre and across laboratories. Sorting methods based on multi-resolution analysis such as wavelet transform are limited by the sampling rate which ultimately limits their widespread application [12], [15]. Representation of spikes in terms of features loses the morphology of the spikes, which is important in invasive studies [12], [15]. New spike sorting methods are needed that address these practical

Manuscript received April 6, 2011. This work was supported by the National Institute of Health/National Institute of Neurological Disorders and Stoke(NIH/NINDS) grant # R01NS058802 and partially supported by the Natural Sciences and Engineering Research Council (NSERC) of Canada under grant # A-7739.

R. Yadav, M. N. S. Swamy, and R. Agarwal are with [1]Center for Signal Processing and Communications (CENSIPCOM), Department of Electrical and Computer Engineering, Concordia University, 1455 de Maisonneuve Blvd. West, Montreal, QC, H3G 1M8, Canada. Email: r_yadav@encs.concordia.ca, swamy@encs.concordia.ca, and ragarwal@leapmedical.ca
A. K. Shah and J. A. Loeb are with the [2]Department of Neurology and the [3]Center for Molecular Medicine and Genetics, Wayne State University School of Medicine, Detroit, Michigan 48201, USA. Email: ashah@med.wayne.edu, and jloeb@med.wayne.edu

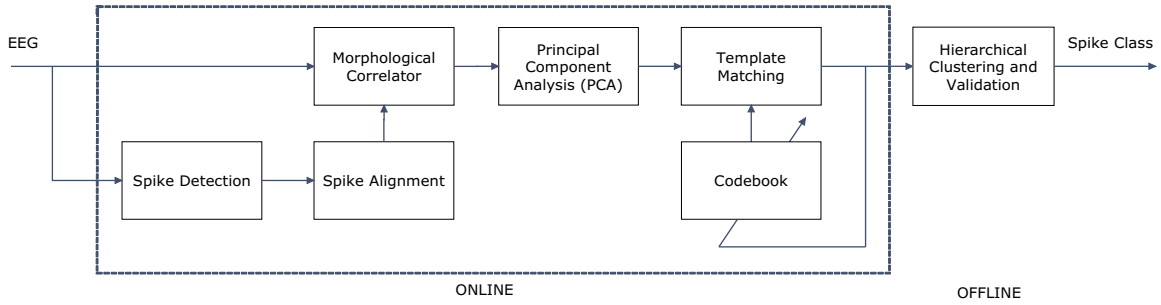

Figure 1. Block diagram of the proposed spike-sorting algorithm.

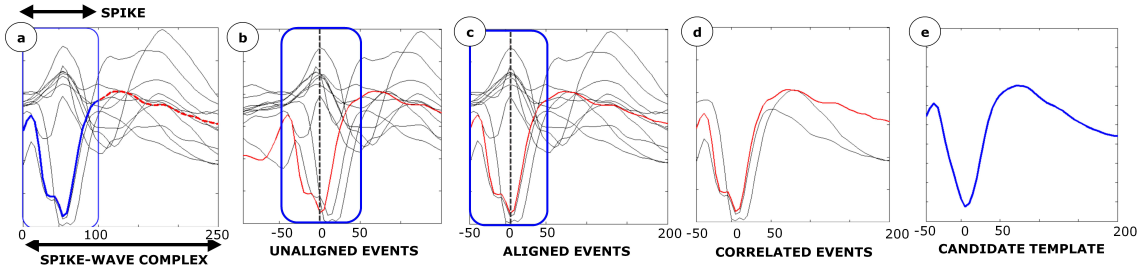

Figure 2. Illustration of spike, spike-wave complex and intermediate stages of the proposed spike sorting algorithm. (**a**) represents multichannel spike and spike-wave complexes. Spike events are in the rectangular ('blue') box in **a-c**. The reference spike (shown by thick 'red' in **a-d**) is the event detected by the spike detector. The spike alignment block aligns multichannel spike event (**b**) w.r.t. the reference spike. The resulting aligned events are shown in (**c**). Morphological correlator retains only spikes similar to the reference spike as seen in (**d**). Spike-wave complex resulting from morphological correlator shown in (**d**) is input to the PCA block to identify candidate template (**e**). Note that number of channels is limited to 11 for illustration, and x-axis represents time in milliseconds.

issues, but without a loss of performance.

Here, we present a novel, computationally light, automatic, patient-specific spike sorting method that assumes no *a priori* knowledge of the spike waveform. The method is not dependent on the sampling rate or number of electrodes. Spike waveform morphologies are retained with dynamically derived spike templates. The method first aligns the multichannel EEG spike apex. A codebook is derived using a morphological correlator, PCA, and template matching of the multichannel spike event. The codebook is updated with every subsequent spike-wave complex (SWC). The update refines an existing SWC template or creates a new class as necessary. Redundant and irrelevant classes in the codebook are removed automatically by the hierarchical clustering and validation module after completing the online analysis. Preliminary results from five patients are presented and reveal well-separated distinct spike classes in the dominant clusters with average retention of 82.1% of the detected spikes.

II. Method

Five patients with medically intractable epilepsy underwent long-term intracranial EEG monitoring between January 2002 and August 2008. The long-term recordings were obtained with subdural grid electrodes varying from 84-128 channels using a Stellate Harmonie digital recorder (Stellate Inc., Montreal, Canada) with a sampling rate of 200 Hz for each channel. For each patient, three distinct 10 minute segments of continuous awake EEG were selected with the following criteria: (a) at least a 3 hours between each segment; and (b) $\geq$ 2 hours after a partial seizure and $\geq$ 8 hours after a secondarily generalized tonic-clonic seizure as described in [4]. One of the three randomly selected 10-minute sections constitutes the training data in this study.

The block diagram of the proposed spike-sorting algorithm is shown in Fig. 1. It is composed of six blocks: (a) spike detection, (b) spike alignment, (c) morphological correlator, (d) principal component analysis, (e) template matching, and (f) hierarchical clustering and validation.

It is important to define various terms used in this paper before describing each of the blocks. **We define spike detected on any specific channel as the reference spike (shown in thick 'red' in Fig.** 2 **a-d), and multichannel EEG centered on the vertex of the reference spike as the multichannel spike event (Fig.** 2 **c).** A variety of clinical studies examine not only the spike but also the waveform following the spike, which we define as the spike-wave complex (SWC) shown in Fig. 2. Since, we use the multichannel spike event, the additional EEG waveform for each channel following the spike constitutes the multichannel SWC. The best representation for a group of SWCs is defined as the template. Codebook is a collection of templates for a patient. The details of each of the six blocks of the proposed methods are described below.

A. Spike Detection

The state-dependent spike detection algorithm in the Stellate Harmonie software v 6.2e (Stellate Inc.) with default settings is utilized to detect spikes in the data [16]. In this paper, even though previously detected spikes are utilized for spike clustering, processing of the data is done in an online fashion. The processing is done sequentially one spike at a time as it would be in the online case. Multichannel EEG around the detected (reference) spike is extracted for the analysis.

B. Spike Alignment

The multichannel EEG is aligned with respect to the reference spike. The multichannel data of Fig. 2b is input to the spike alignment block that corrects the misalignment in the spike apex by examining local maxima and minima within ± 25 ms of the reference vertex. The aligned multichannel spike waveform of 100 ms length (± 50 ms around the corrected spike vertex) is defined as multichannel spike event $\mathbf{X} \in R^{nxm}$, where *n* is the number of channels of length *m* (Fig. 2c).

C. Morphological Correlator

The aligned multichannel spike event $\mathbf{X}$ and the reference spike (Fig. 2c) is input to the morphological correlator. This step identifies spikes similar to the reference spike among the other channels. To do so, correlation coefficient ρ_{ij} defined by (1) is computed, where $i = 1, \ldots, n$ and j is the reference spike. Spikes similar to the reference spike are identified by comparing ρ_{ij} to a threshold ρ_{MC} (Fig. 2d). A correlation coefficient greater than $\rho_{MC} = 0.7$ is considered suitable to identify similar spikes. This step reduces the number of channels and is similar to subtractive clustering [6] resulting in the multichannel SWC event $\mathbf{Y} \in R^{nxk}$, where *n* is the number of channels of length *k* ($\geq m$). The length of SWC *k* is 250 ms that includes spike and 150 ms waveform following the spike is considered suitable for this study.

$$\rho_{ij} = \frac{n\Sigma x_i x_j - (\Sigma x_i)(\Sigma x_j)}{\sqrt{n(\Sigma x_i^2) - (\Sigma x_i)^2}\sqrt{n(\Sigma x_j^2) - (\Sigma x_j)^2}} \quad (1)$$

D. Principal Component Analysis (PCA)

PCA is used to extract the principal components from the multichannel SWC $\mathbf{Y}$,

$$\mathbf{Y} = SL^T, \quad (2)$$

where *L* is the principal component loading matrix and *S* the principal component scores matrix [6]. In this study, we use the first principal component as the candidate spike-wave complex (Fig. 2e) for the template matching. This block increases the signal-to-noise ratio of the SWC while preserving the SWC morphology and reducing the data dimensionality. Note that PCA seeks directions (principal directions) that best represent the original data. Identifying spikes similar to the reference spike using morphological correlator reduces the computational complexity and always directs the principal component (first component) towards the reference spike.

E. Codebook-based Template-matching

The codebook stores SWC templates, class membership details such as time and channel of occurrence, and various properties of the individual SWCs. The *i*th candidate spike-waveform complex (C_i) is matched with the templates in the codebook. The template matching is correlation-based, and best match to the C_i is identified by (1). The template matching threshold ρ_{TM} is set to 0.9. The template is updated by taking average of the C_i with the best matching template in the codebook. However, if no suitable match to C_i is found, the codebook is appended with a new class.

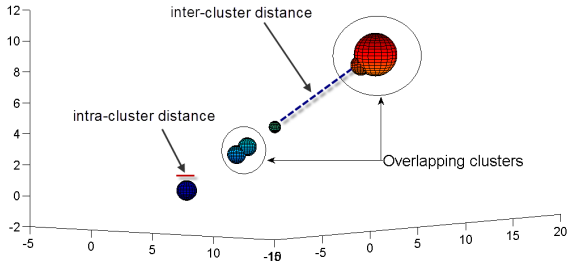

Figure 3. Visual cluster analysis

F. Hierarchical Clustering and Validation

This block examines codebook in the offline mode when all spikes in the data have been classified. Overlapping clusters and insignificant templates (due to noise) are identified with this strategy. The bottom-up (agglomerative) hierarchical clustering is utilized to identify and merge overlapping clusters. The process iterates until all objects are aggregated into a single class using the minimum distance linkage rule where the similarity parameter is the Mahalanobis distance. This approach allows good separation of the clusters.

Rarely occurring SWC events are deleted from the codebook by applying a threshold relative to the highest-ranking template (template with the highest number of members). The threshold is set to 10% obtained from receiver operating characteristic curve.

III. Results

One of the main challenges in the spike sorting is the lack of *a priori* knowledge of the total number of spike classes in the recording. Analyzing cluster quality thus becomes very difficult. Codebook quality is assessed by inter- and intra-cluster distance measures. These measures are projected on a 3-dimensional plot that provides appealing and easy-to-interpret visual cluster analysis (see Fig. 3). The example depicts 3D projection of inter- and intra- cluster distance before hierarchical clustering. It illustrates that the proposed spike-sorting method resulted in six clusters of which four are well separated compact clusters while two clusters overlap. Overlapping clusters are identified and merged by the hierarchical clustering and validation block. The output resulting from the hierarchical clustering blocks are both compact and disjoint.

The spike-sorting results were visually examined for the number of overlapping clusters (Table 1). Visual examination of the codebook and 3D cluster quality plot confirmed distinct and compact clusters for all five patients. An example of the codebook for Patient #3 is shown in Fig. 4. The codebook contains three significant spike classes obtained by the proposed spike-sorting algorithm. The templates are shown in 'red' superimposed over its members (Fig. 4A). The cluster quality plot depicts (Fig. 4B) disjoint and well-separated clusters. We also generated dendrogram plot of the codebook to examine separation between the clusters (Fig. 4C). The dendrogram plot is generated by a bottom-up complete

Table I
CODEBOOK ANALYSIS

PID	TS	TSC	TOC	SL (%)	TIC	SPIC
1	7934	2	-	19.9	182	8.7
2	3191	5	-	26.2	152	5.5
3	1296	3	-	10.5	48	6.5
4	10959	4	-	17.1	116	16.1
5	10495	6	-	15.6	100	3.8
			Average	**17.9**	**120**	**8**

PID = Patient index, TS = total number of spikes detected, TSC = total number of significant clusters, TOC = total number of overlapping clusters, SL = percentage of spikes lost, TIC = total number of insignificant clusters (rejected clusters), and SPIC = average number of spikes in the rejected clusters.

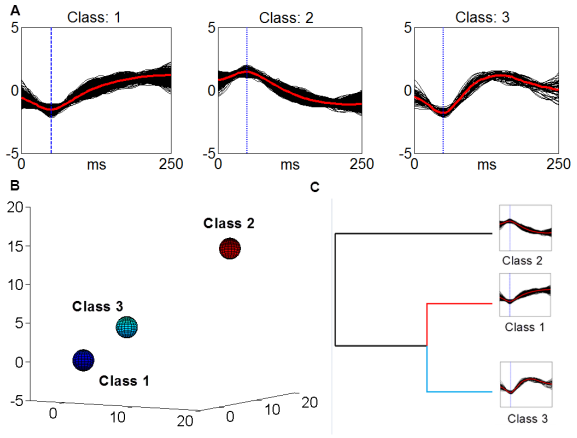

Figure 4. Example of dynamic codebook obtained by the proposed system for Patient #3. (A) represents the template and its member. The template is shown in 'red'. (B) presents the projection inter- and intra- cluster distance on to a 3D plot that allows rapid examination of cluster quality. No overlapping or closely-spaced clusters are seen in this data. (C) depicts the dendogram mapping of the codebook. This is a secondary approach to examine codebook quality. Class 1 and Class 3 templates are similar to each other in the spike waveform. However, the wave complex following the spike are different. The two classes are placed at the same node based on the similarity measure in the dendogram.

linkage rule with Euclidean distance. This secondary approach also allows scrutinizing the cluster quality.

Spikes originating from the same brain region tend to have same morphology and will be retained in the significant clusters resulting from the sorting algorithm. The proposed sorting algorithm retains 82.1% of the automatically detected spikes. All of the resulting clusters (significant) were disjoint and compact (Table I). On average, the method rejects 17.9% of the total detected spikes that were distributed across 120 clusters per patient. The average number of spikes in each of the insignificant clusters was approximately 8 compared to 1570 in the significant clusters. A majority of the rejected clusters were due to either artifact events or were rarely occurring events.

IV. SUMMARY

In this paper, a new multichannel spike sorting method with a dynamic patient-specific codebook is presented. The method builds the codebook without any *a priori* knowledge about the spikes. Our method performs spike sorting using the spike waveform that combines a simple spike alignment technique, a morphological correlator, PCA, and template matching to generate the patient-specific codebook. To address the problem of overlapping and redundant classes in the codebook, hierarchical clustering is performed at the completion of classification, resulting in compact and non-overlapping classes. The method was optimized using multichannel subdural EEG recordings from 5 patients. For each patient, the classification results were visually screened. The resulting codebook retained 82% of the detected spikes in disjoint and well-separated clusters reflecting robustness of the proposed method. Future work will require validation of the cluster quality by various techniques, comparison of the method against other published methods for spike sorting, and most importantly clinical validation of the clusters by trained electrophysiologists.

REFERENCES

[1] S. Demont-Guignard, P. Benquet, U. Gerber, and F. Wendling, "Analysis of intracerebral eeg recordings of epileptic spikes: Insights from a neural network model," *IEEE Transactions on Biomedical Engineering*, vol. 56, no. 12, pp. 2782–2795, 2009.

[2] E. D. Marsh, B. Peltzer, r. Brown, M. W., C. Wusthoff, J. Storm, P. B., B. Litt, and B. E. Porter, "Interictal eeg spikes identify the region of electrographic seizure onset in some, but not all, pediatric epilepsy patients," *Epilepsia*, vol. 51, no. 4, pp. 592–601, 2010.

[3] C. E. Stafstrom, "Sites of interictal spike generation in neocortex," *Epilepsy currents / American Epilepsy Society*, vol. 4, no. 3, pp. 96–7, 2004.

[4] S. N. Rakhade, A. K. Shah, R. Agarwal, B. Yao, E. Asano, and J. A. Loeb, "Activity-dependent gene expression correlates with interictal spiking in human neocortical epilepsy," *Epilepsia*, vol. 48 Suppl 5, pp. 86–95, 2007.

[5] S. N. Rakhade and J. A. Loeb, "Focal reduction of neuronal glutamate transporters in human neocortical epilepsy.," *Epilepsia*, vol. 49, pp. 226–236, Feb 2008.

[6] P. Zhang, "Spike sorting based on automatic template reconstruction with a partial solution to the overlapping problem," *Journal of Neuroscience Methods*, vol. 135, no. 1-2, pp. 55–65, 2004.

[7] E. N. Brown, R. E. Kass, and P. P. Mitra, "Multiple neural spike train data analysis: state-of-the-art and future challenges," *Nature neuroscience*, vol. 7, no. 5, pp. 456–61, 2004.

[8] H. Kaneko, H. Tamura, and S. S. Suzuki, "Tracking spike-amplitude changes to improve the quality of multineuronal data analysis," *IEEE Transactions on Biomedical Engineering*, vol. 54, no. 2, pp. 262–272, 2007.

[9] R. Vollgraf and K. Obermayer, "Improved optimal linear filters for the discrimination of multichannel waveform templates for spike-sorting applications," *IEEE Signal Processing Letters*, vol. 13, no. 3, pp. 121–124, 2006.

[10] M. T. Wolf and J. W. Burdick, "A bayesian clustering method for tracking neural signals over successive intervals," *IEEE Transactions on Biomedical Engineering*, vol. 56, no. 11, pp. 2649–2659, 2009.

[11] D. Ge, E. Le Carpentier, J. Idier, and D. Farina, "Spike sorting by stochastic simulation," *IEEE Transactions on Neural Systems and Rehabilitation Engineering*, vol. 19, no. 3, pp. 249–259, 2011.

[12] Y. Ghanbari, P. E. Papamichalis, and L. Spence, "Graph-laplacian features for neural waveform classification," *IEEE Transactions on Biomedical Engineering*, vol. 58, no. 5, pp. 1365–1372, 2011.

[13] H.-P. Kriegel, P. Kröger, and A. Zimek, "Clustering high-dimensional data: A survey on subspace clustering, pattern-based clustering, and correlation clustering," *ACM Trans. Knowl. Discov. Data*, vol. 3, pp. 1:1–1:58, March 2009.

[14] T. Takekawa, Y. Isomura, and T. Fukai, "Accurate spike sorting for multi-unit recordings.," *Eur J Neurosci*, vol. 31, pp. 263–272, Jan 2010.

[15] H.-L. Chan, T. Wu, S.-T. Lee, M.-A. Lin, S.-M. He, P.-K. Chao, and Y.-T. Tsai, "Unsupervised wavelet-based spike sorting with dynamic codebook searching and replenishment," *Neurocomputing*, vol. 73, no. 7-9, pp. 1513–1527, 2010.

[16] J. Gotman and L. Y. Wang, "State-dependent spike detection: concepts and preliminary results.," *Electroencephalogr Clin Neurophysiol*, vol. 79, pp. 11–19, Jul 1991.